



Photocatalytic conversion of CO₂ in water over Ag-modified La₂Ti₂O₇

Zheng Wang^a, Kentaro Teramura^{a,b,c,*}, Saburo Hosokawa^{a,b}, Tsunehiro Tanaka^{a,b,**}

^a Department of Molecular Engineering, Graduate School of Engineering, Kyoto University, Kyoto 615-8510, Japan

^b Elements Strategy Initiative for Catalysts & Batteries (ESICB), Kyoto University, 1-30 Goryo-Ohara, Nishikyo-ku, Kyoto 615-8245, Japan

^c Precursory Research for Embryonic Science and Technology (PRESTO), Japan Science and Technology Agency (JST), 4-1-8 Honcho, Kawaguchi, Saitama 332-0012, Japan



ARTICLE INFO

Article history:

Received 16 May 2014

Received in revised form 20 July 2014

Accepted 25 July 2014

Available online 12 August 2014

Keywords:

Conversion of CO₂ to CO

La₂Ti₂O₇ photocatalyst

Evolution of O₂

Isotope labeling

ABSTRACT

We have found that Ag-modified La₂Ti₂O₇ with a layered perovskite structure exhibits activity for the photocatalytic conversion of CO₂ to CO in pure water. The evolution of O₂ proves that H₂O works as an electron donor for the photocatalytic conversion of CO₂. CO was generated as the main product, and CO, H₂, and O₂ were produced in stoichiometric amounts. The crystallite size of La₂Ti₂O₇ increased and the surface area decreased with increasing calcination temperature and time. Maximization of the photocatalytic activity of La₂Ti₂O₇ was accomplished by making a trade-off between the crystallite size and surface area. In addition, the loading amount and modification method of the Ag cocatalyst also influenced the amount of CO evolved. An isotope labeling experiment using ¹³CO₂ confirmed that the origin of evolved CO was not the residual carbon species on the La₂Ti₂O₇ surface, but was rather the CO₂ gas that was introduced during the experimental process.

© 2014 Elsevier B.V. All rights reserved.

1. Introduction

Due to the increased rates of deforestation and combustion of fossil fuels, CO₂ greenhouse gas emissions in the atmosphere is increasingly becoming an environmental hazard due to an accelerated rise in global temperatures [1,2]. Therefore, it is essential to not only control the level of CO₂ emissions, but to devise strategies to effectively remove CO₂ from the atmosphere. Among the various strategies for reducing the concentration of CO₂, the catalytic conversion of CO₂ to liquid fuels and chemicals is appealing due to the utilization of CO₂ as a natural derivative for production [3,4]. However, elevated temperature-pressure processes require a significant input of energy. Using solar light as an ideal and abundant energy source, it is possible to devise a promising route for the photocatalytic conversion of CO₂ into useful chemical products such as CO, HCOOH, HCHO, CH₃OH, and CH₄ under ambient temperature and pressure conditions [5,6].

The photocatalytic conversion of CO₂, an example of artificial photosynthesis, is a thermodynamically uphill reaction that utilizes photo-generated electrons as a source of energy [7]. It is difficult to achieve the reduction of CO₂ by H₂O over heterogeneous photocatalysts due to the competing generation of H₂ gas from the overall splitting of water [8]. Moreover, a stoichiometric amount of evolved O₂ should also be obtained if H₂O functions as an electron donor during the photocatalytic conversion of CO₂. Although various photocatalysts such as TiO₂ [9,10], CdS [11], BiVO₄ [12], and ZnGa₂O₄ [13] have been reported for the reduction of CO₂ in H₂O, the evolution of O₂ was not observed in the reaction, implying that the consumption of photogenerated holes is ambiguous. Until recently, Kudo et al. have discovered the photocatalytic conversion of CO₂ by H₂O over Ag-modified ALa₄Ti₄O₁₅ (A = Ca, Sr, and Ba), where the amount of evolved CO was higher than the amount of evolved H₂, and a stoichiometric amount of O₂ was also simultaneously observed [14].

It is known that La-Ti based oxide materials with a layered perovskite structure can efficiently decompose H₂O into H₂ and O₂ without any sacrificial reagents under UV light irradiation [15–18]. Among La-Ti oxides, La₂Ti₂O₇, which possesses a (110) plane-type perovskite structure, was reported to show good photocatalytic activity for overall water splitting [15,16,18]. Since the reduction of CO₂ requires a reduction potential higher than that for H⁺, the wide bandgap of La₂Ti₂O₇, which is capable of generating photoelectrons with a high reduction potential, should result in the efficient reduction of CO₂. In order to obtain a high crystallinity and surface area

* Corresponding author at: Department of Molecular Engineering, Graduate School of Engineering, Kyoto University, Kyoto 615-8510, Japan.
Tel.: +81 75 383 2559; fax: +81 75 383 2561.

** Corresponding author at: Department of Molecular Engineering, Graduate School of Engineering, Kyoto University, Kyoto 615-8510, Japan.
Tel.: +81 75 383 2558; fax: +81 75 383 2561.

E-mail addresses: teramura@molenk.kyoto-u.ac.jp (K. Teramura), tanakat@molenk.kyoto-u.ac.jp (T. Tanaka).

at low calcination temperature, we used a polymerized complex method over the typical solid state reaction method to prepare $\text{La}_2\text{Ti}_2\text{O}_7$ [15,18]. In this study, $\text{La}_2\text{Ti}_2\text{O}_7$ was fabricated using the polymerized complex method, and the photocatalytic conversion of CO_2 by H_2O over Ag-modified $\text{La}_2\text{Ti}_2\text{O}_7$ was investigated.

2. Experimental

$\text{La}_2\text{Ti}_2\text{O}_7$ was fabricated using a polymerized complex method, where a defined amount of titanium tetraisopropoxide ($\text{Ti}[\text{OCH}(\text{CH}_3)_2]_4$, 95.0%, Wako) was dissolved in 0.2 mol of ethylene glycol ($\text{C}_2\text{H}_6\text{O}_2$, 99.5%, Wako) at room temperature. 0.3 mol of anhydrous citric acid ($\text{C}_6\text{H}_8\text{O}_7$, 98.0%, Wako) was then added and the mixture was heated with continuous stirring at 333 K. After the complete dissolution of citric acid, an appropriate amount of lanthanum nitrate ($\text{La}(\text{NO}_3)_3 \cdot 6\text{H}_2\text{O}$, 99.9%, Wako) and 20 mL of methanol were added into the above solution. The additive ratio between $\text{La}(\text{NO}_3)_3$ and $\text{Ti}[\text{OCH}(\text{CH}_3)_2]_4$ was 1:1. The mixture was heated at 403 K for 3 h to obtain a transparent gel without any precipitated solid. The viscous gel was pyrolyzed at 623 K to remove all carbon-containing compounds, and the resulting powder precursor was calcined from 1173 to 1423 K for 1–8 h in static air. The Ag cocatalyst was chemically modified on $\text{La}_2\text{Ti}_2\text{O}_7$ through a series of chemical reduction, impregnation, and photodeposition methods. In the chemical reduction method, an aqueous NaPH_2O_2 solution was added into 100 mL of a suspension of photocatalysts (2.0 g) containing AgNO_3 . After stirring at 333 K for 2 h, the modified photocatalyst was washed with deionized water three times and dried under vacuum at room temperature. In the impregnation method, photocatalysts were homogeneously dispersed in an aqueous AgNO_3 solution. The solution was then evaporated, dried, and calcinated at 723 K in a stream of dry air for 2 h. The photodeposition method was employed in situ during the photocatalytic conversion of CO_2 . The structure and crystallinity of $\text{La}_2\text{Ti}_2\text{O}_7$ samples were characterized by X-ray diffraction (XRD) using a Rigaku Multi Flex powder X-ray diffractometer. The UV-vis diffused reflectance spectra (UV-vis DRS) were measured by a JASCO Corporation V-670 spectrometer equipped with an integrating sphere. Spectralon®, supplied by Labsphere Inc., was used as a standard reflection sample. The Brunauer–Emmett–Teller (BET) surface area was measured by N_2 adsorption at 77 K using a volumetric gas adsorption apparatus (BELmini, Bel Japan, Inc.). The Ag K-edge (25.5 keV) X-ray absorption fine structure (XAFS) measurements were made in the fluorescence mode at the BL01B1 beamline of the SPring-8 synchrotron radiation facility (Hyogo, Japan). The spectra were reduced by a Rigaku REX2000 program Ver. 2.5.9 (Rigaku Corp.). TEM images were obtained with a JEOL JEM-1400 transmission electron microscope (TEM) operating at an accelerating voltage of 120 kV.

The photocatalytic reaction was carried out in a flow system using an inner-irradiation-type reaction vessel at room temperature and ambient pressure. The photocatalyst (1.0 g) was dispersed in ultra-pure water (1.0 L), and CO_2 (99.999%) was bubbled into the water at a flow rate of 30 mL min^{-1} . The suspension was irradiated under a 400 W high-pressure mercury lamp with a quartz filter connected to a cooling water system. Generated gaseous products such as H_2 , O_2 , and CO were analyzed by thermal conductivity detector-gas chromatography (TCD-GC) using a GC-8A chromatograph (Shimadzu Corp.) equipped with a Molecular Sieve 5A column (carrier gas: Ar) and by flame ionization detector-gas chromatography (FID-GC) using a methanizer and a Shincarbon ST column (carrier gas: N_2). In the isotope labeling reaction using $^{13}\text{CO}_2$, an inner-irradiation-type reaction vessel was connected to a closed circulating system with a vacuum line. The prepared Ag-modified $\text{La}_2\text{Ti}_2\text{O}_7$ sample (500 mg) was dispersed in ultrapure

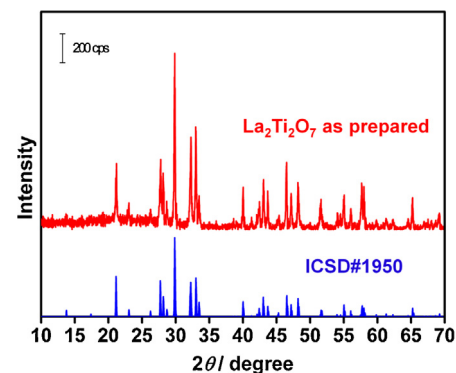


Fig. 1. XRD patterns of $\text{La}_2\text{Ti}_2\text{O}_7$ fabricated by polymerized complex method with calcination at 1373 K for 4 h.

water (350 mL). $^{13}\text{CO}_2$ (2000 mmol), which was purified by vacuum distillation at liquid- N_2 temperature, was introduced into the reactor, and the suspension was irradiated by a 400 W high-pressure mercury lamp through a quartz filter connected to a cooling water system. The formation of either ^{13}CO or ^{12}CO after 5.5 h was analyzed by a quadrupole-type mass spectrometer (BELJapan, Inc., BEL Mass) combined with a TCD-GC (Carrier gas: Ar).

3. Results and discussion

Fig. 1 shows the XRD patterns of $\text{La}_2\text{Ti}_2\text{O}_7$, which was prepared using the polymerized complex method with subsequent calcination at 1373 K for 4 h. In accordance with the standard pattern (ICSD#1950), $\text{La}_2\text{Ti}_2\text{O}_7$ exhibits a layered perovskite structure, which consists of perovskite-like slabs with a thickness equivalent to four corner-linked (TiO_6) octahedra. The edge of the TiO_6 octahedra is exposed to the interlayers of $\text{La}_2\text{Ti}_2\text{O}_7$, which run parallel to the (110) plane of the bulk perovskite slabs to give a (110) plane-type perovskite structure [18]. Fig. 2 shows the UV-vis DRS of $\text{La}_2\text{Ti}_2\text{O}_7$ after conversion of the reflection coefficient, R , to the absorption coefficient, $F(R_\infty)$, through the Kubelka–Munk function, $F(R_\infty) = (1 - R^2)/2R$. The bandgap energy was derived from Davis–Mott's equation, $\alpha h\nu = (h\nu - E_g)^n$, where α is the absorption coefficient; $h\nu$ is the energy of the irradiated light; and E_g is the bandgap energy. n is an experimental value, where the values for indirect allowed, indirect forbidden, direct allowed, and direct forbidden transitions are 2, 3, 1/2, and 3/2, respectively [19]. As shown in the inset of Fig. 2, this equation ($n=1/2$, direct allowed

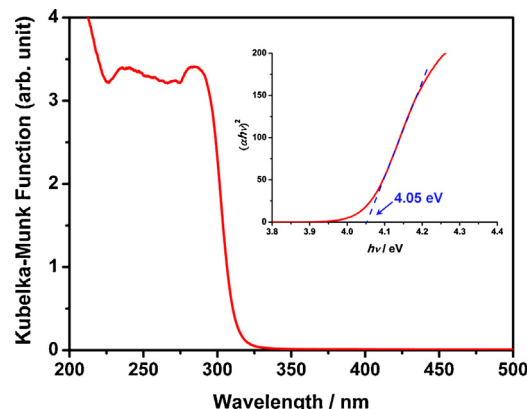


Fig. 2. UV-vis DRS of $\text{La}_2\text{Ti}_2\text{O}_7$ prepared by polymerized complex method with calcination at 1373 K for 4 h. Inset: The plots of $(\alpha h\nu)^2$ versus the energy of light ($h\nu$) afford the band gap energy for $\text{La}_2\text{Ti}_2\text{O}_7$.

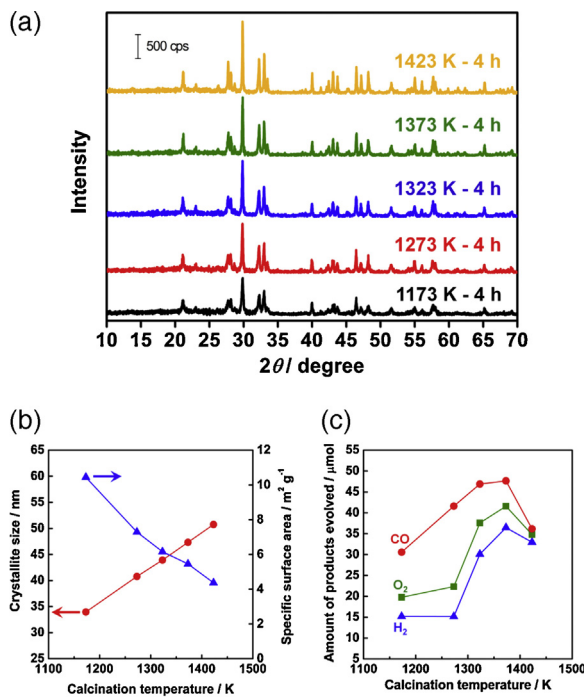


Fig. 3. (a) XRD patterns of $\text{La}_2\text{Ti}_2\text{O}_7$ at various calcination temperature. (b) Crystallite size and specific surface area of $\text{La}_2\text{Ti}_2\text{O}_7$ at various calcination temperature. (c) Evolution of CO (circle), O_2 (square), and H_2 (triangle) in 7 h over $\text{La}_2\text{Ti}_2\text{O}_7$ calcined at various temperature for 4 h. Ag cocatalyst was modified by chemical reduction method and the loading amount was 1 wt%.

transition), gives an estimated value of 4.05 eV for the bandgap energy of $\text{La}_2\text{Ti}_2\text{O}_7$.

Fig. 3a shows XRD patterns of a sample of $\text{La}_2\text{Ti}_2\text{O}_7$ that was treated at temperatures ranging from 1173 to 1423 K. All samples exhibited the layered perovskite structure of $\text{La}_2\text{Ti}_2\text{O}_7$ without any impurity phases, which indicates that calcination above 1173 K following the polymerized complex procedure successfully caused crystallization of $\text{La}_2\text{Ti}_2\text{O}_7$. It has already been reported that crystalline $\text{La}_2\text{Ti}_2\text{O}_7$ was obtained by calcination above 1173 K, and that the photocatalytic activity of $\text{La}_2\text{Ti}_2\text{O}_7$ calcined below 1173 K was almost negligible [18]. In addition, all the peaks in the XRD patterns of $\text{La}_2\text{Ti}_2\text{O}_7$ became sharper and higher with an increase in the calcination temperature. The crystallite size of $\text{La}_2\text{Ti}_2\text{O}_7$ could be obtained using the FWHM (Full Width of Half Maximum) of XRD peaks, based on Scherrer's equation. As shown in Fig. 3b, the crystallite size of $\text{La}_2\text{Ti}_2\text{O}_7$ calcined at temperatures ranging from 1173 to 1423 K increased linearly from 34.0 to 50.8 nm. On the other hand, the specific surface area of $\text{La}_2\text{Ti}_2\text{O}_7$, measured by the BET method, decreased when the calcination temperature was elevated (Fig. 3b). These results mean that calcination at various high temperatures affects not only the crystallite size, but also the specific surface area of $\text{La}_2\text{Ti}_2\text{O}_7$. Since photocatalytic activity is dependent on the crystallinity and surface area of the photocatalyst, the activities of $\text{La}_2\text{Ti}_2\text{O}_7$ calcined at various temperatures were monitored to compare the photocatalytic conversion of CO_2 by H_2O under UV irradiation. All the samples were modified with Ag using the chemical reduction method. Fig. 3c shows the amount of CO, O_2 , and H_2 evolved in 7 h. CO was evolved as the main reduction product, and a significantly smaller yield of evolved H_2 was observed. The simultaneous evolution of O_2 indicated that H_2O worked as an electron donor to consume the holes generated during the photocatalytic conversion of CO_2 . Increasing the calcination temperature of $\text{La}_2\text{Ti}_2\text{O}_7$ from 1173 to 1373 K caused an increase in the activity for the photocatalytic conversion of CO_2 . This can be attributed to the high crystallinity of $\text{La}_2\text{Ti}_2\text{O}_7$ in spite of the decrease in the

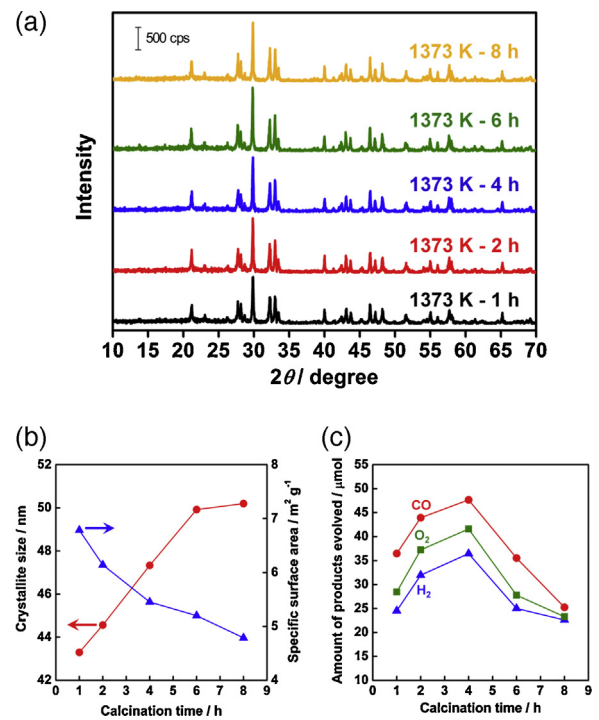


Fig. 4. (a) XRD patterns of $\text{La}_2\text{Ti}_2\text{O}_7$ calcined at 1373 K for different time. (b) Crystallite size and specific surface area of $\text{La}_2\text{Ti}_2\text{O}_7$ calcined at 1373 K for different time. (c) Evolution of CO (circle), O_2 (square), and H_2 (triangle) in 7 h over $\text{La}_2\text{Ti}_2\text{O}_7$ calcined at 1373 K for different time. Ag cocatalyst was modified by chemical reduction method and the loading amount was 1 wt%.

specific surface area. The maximum amount of CO evolved was observed over $\text{La}_2\text{Ti}_2\text{O}_7$ calcined at 1373 K. However, the activity of $\text{La}_2\text{Ti}_2\text{O}_7$ declined upon calcination at temperatures higher than 1373 K.

The calcination time also influences the crystallinity and surface area of $\text{La}_2\text{Ti}_2\text{O}_7$. As shown in Fig. 4a, $\text{La}_2\text{Ti}_2\text{O}_7$ samples that were calcined at 1373 K for 1–8 h experienced an increase in peak intensities in the XRD pattern for each sample. The crystallinity of $\text{La}_2\text{Ti}_2\text{O}_7$ grew with longer calcination times, whereas the BET surface area was reduced (Fig. 4b). As seen with varied calcination temperature, changes in calcination time from 1 to 8 h also influence the activity of $\text{La}_2\text{Ti}_2\text{O}_7$. $\text{La}_2\text{Ti}_2\text{O}_7$ that was calcined at 1373 K for 4 h possessed a crystallite size of 47.3 nm and a specific surface area of 5.5 m^2/g to afford the highest activity for the photocatalytic conversion of CO_2 by H_2O . Generally, a high specific surface area and crystallinity

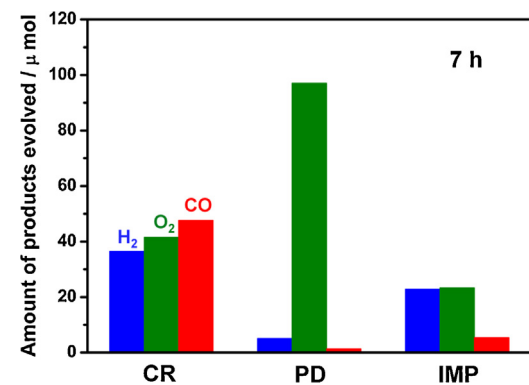


Fig. 5. Amount of evolved gases for the photocatalytic reduction of CO_2 in 7 h over Ag -modified $\text{La}_2\text{Ti}_2\text{O}_7$ prepared by CR (chemical reduction method), PD (photodeposition method), and IMP (impregnation method). $\text{La}_2\text{Ti}_2\text{O}_7$ was calcined at 1373 K for 4 h and the loading amount of Ag was 1 wt%.

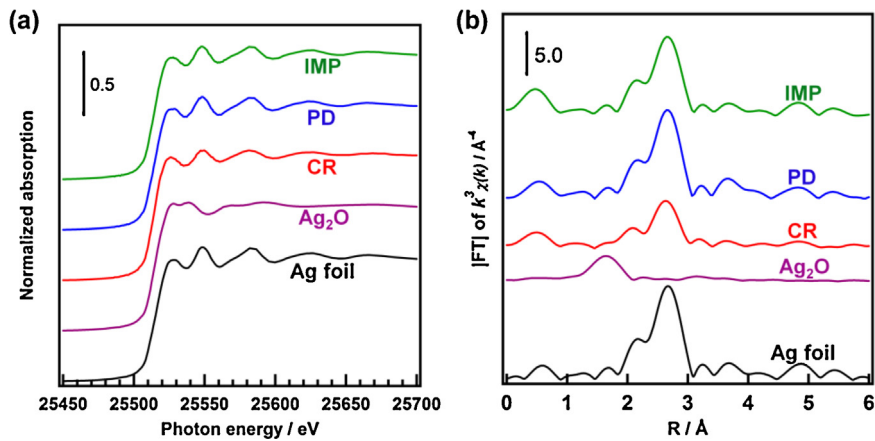


Fig. 6. Ag K-edge XANES (a) and Fourier transformed EXAFS (b) spectra of the Ag-modified $\text{La}_2\text{Ti}_2\text{O}_7$ prepared by chemical reduction method (CR), photodeposition method (PD), impregnation method (IMP). Ag foil and Ag_2O were references. $\text{La}_2\text{Ti}_2\text{O}_7$ was calcined at 1373 K for 4 h and the loading amount of Ag was 1 wt%.

are essential for an efficient heterogeneous photocatalyst. This is because the photocatalytic reaction occurs mostly on the surface of the photocatalyst, and the high crystallinity of the photocatalyst allows a smooth charge separation. Unfortunately, fabrication conditions such as calcination temperature and time can only promote high crystallization of the photocatalyst at the expense of a diminished surface area. This inverse relationship needs to be fine-tuned in order to maximize photocatalytic activity.

In the electrochemical reduction of CO_2 , it has been proven that metallic Ag functions as an effective electrode for the conversion of CO_2 to CO [20]. In the case of the photocatalytic conversion of CO_2 by H_2O , the introduction of an Ag cocatalyst plays an important role in generating CO. In comparison with impregnation and in situ photo deposition methods, Fig. 5 shows that Ag species prepared by the chemical reduction method significantly enhanced the photocatalytic activity for the conversion of CO_2 to CO. This result indicates that the structure of the Ag cocatalyst on the

surface of $\text{La}_2\text{Ti}_2\text{O}_7$ is highly dependent on the modification method. The UV-vis DRS of Ag-modified $\text{La}_2\text{Ti}_2\text{O}_7$ loaded by various methods (Figure S1) showed the same intrinsic absorption as that of bare $\text{La}_2\text{Ti}_2\text{O}_7$. Different surface plasmon absorption in the visible and near-infrared region could be observed for the three samples due to the different particle size and dispersion of Ag cocatalysts. [14,21] The Ag K-edge XANES and Fourier-transformed Ag K-edge EXAFS spectra of Ag-modified $\text{La}_2\text{Ti}_2\text{O}_7$ prepared by the three methods are shown in Fig. 6, of which Ag foil and Ag_2O were used as references. The similar XANES spectra of the three samples and Ag foil clearly proves that Ag species modified by the three methods are metallic Ag. This means the photocatalytic activity is not affected by the chemical state of Ag cocatalyst. Otherwise the Ag–Ag shell intensity of Ag species prepared by the chemical reduction method is much lower than those of Ag species fabricated by the impregnation and photodeposition methods in the FT of EXAFS spectra, which indicates the particle size of Ag cocatalysts in the

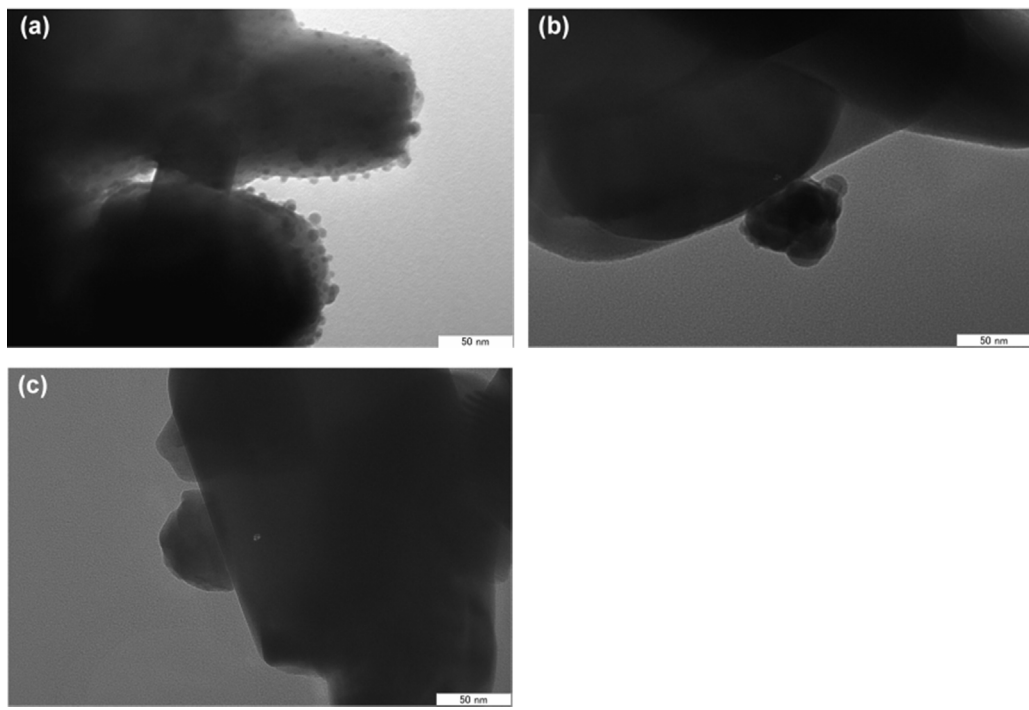


Fig. 7. TEM images of Ag-modified $\text{La}_2\text{Ti}_2\text{O}_7$ prepared by chemical reduction (a), photodeposition (b), and impregnation (c) methods. $\text{La}_2\text{Ti}_2\text{O}_7$ was calcined at 1373 K for 4 h and the loading amount of Ag was 1 wt%.

Table 1

Effect of Ag content on the photocatalytic conversion of CO₂. La₂Ti₂O₇ was calcined at 1373 K for 4 h. Ag cocatalyst was modified by chemical reduction method.

Loading amount	Activity ($\mu\text{mol h}^{-1}$)			Reacted electrons ($\mu\text{mol h}^{-1}$)	Reacted holes ($\mu\text{mol h}^{-1}$)
	H ₂	O ₂	CO		
0 wt%	2.7	2.3	0.8	7.0	9.2
0.5 wt%	4.9	5.2	4.6	19	21
1.0 wt%	4.9	5.3	5.2	20	21
1.5 wt%	4.3	4.8	4.3	17	19
2.0 wt%	3.9	4.4	4.1	16	18

chemical reduction sample is the smallest among the three samples. Fig. 7 represents TEM images of Ag-modified La₂Ti₂O₇ loaded by the three methods. Actually, Ag nanoparticles prepared by the chemical reduction method are highly dispersed on the surface of La₂Ti₂O₇ with the particle size between 2 and 10 nm. In contrast, the wet impregnation and photodeposition methods result in the aggregation of Ag particles and poor Ag dispersion on La₂Ti₂O₇. It is noted that the formation of metallic Ag nanoparticles with the small size and uniform distribution by the chemical reduction method caused the enhancement for the photocatalytic conversion of CO₂ in water.

Table 1 shows the photocatalytic activity of Ag-modified La₂Ti₂O₇ prepared by the chemical reduction method with various loading amounts of Ag. While conversion of CO₂ could occur on

bare La₂Ti₂O₇, the evolution rate of H₂ (2.7 $\mu\text{mol h}^{-1}$) was higher than that of CO (0.8 $\mu\text{mol h}^{-1}$). This is because conversion of CO₂ competes with the splitting of water at an insufficient number of suitable reaction sites on bare La₂Ti₂O₇. Modification of La₂Ti₂O₇ with an Ag cocatalyst caused a dramatic increase in the photocatalytic activity for CO evolution. While the evolution rate of CO increased with the addition of larger amounts of Ag ranging from 0 to 1.0 wt%, the rate declined with higher amounts of Ag. The maximum activity was obtained for La₂Ti₂O₇ with 1 wt% of the Ag cocatalyst. It is clear that the modification by the Ag cocatalyst provided enough catalytic sites for the reduction of CO₂ on the surface of La₂Ti₂O₇, and the conversion of CO₂ to CO took precedence over H₂ production at such sites. In addition, the evolution of H₂ was also improved through the introduction of the Ag cocatalyst, possibly owing to the promotion of electron–hole separation. The Ag cocatalyst efficiently captures the photogenerated electrons and supplies them for the reductions of both CO₂ and H⁺. Any remaining

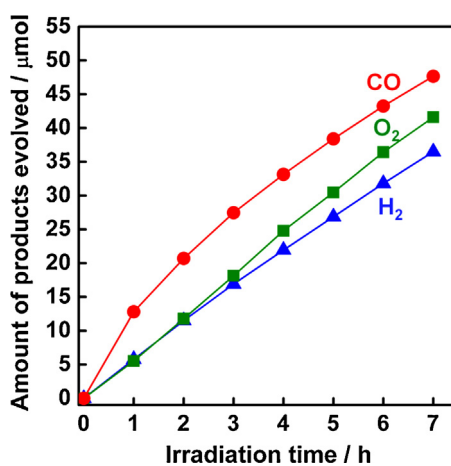


Fig. 8. Time courses of CO (circle), O₂ (square), and H₂ (triangle) evolved for the photocatalytic conversion of CO₂ in water over Ag-modified La₂Ti₂O₇. La₂Ti₂O₇ was calcined at 1373 K for 4 h. Ag cocatalyst was modified by chemical reduction method and the loading amount was 1 wt%.

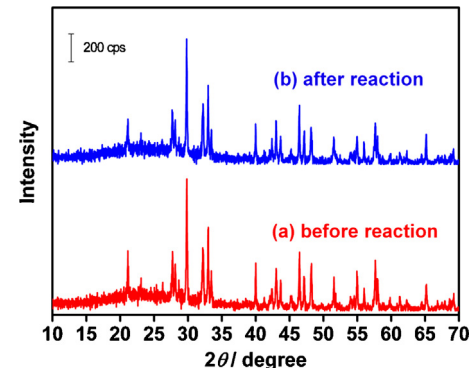


Fig. 10. XRD patterns of La₂Ti₂O₇ (a) before and (b) after the reaction. La₂Ti₂O₇ was synthesized by polymerized complex method and calcined at 1373 K for 4 h. Ag cocatalyst was modified by chemical reduction method and the loading amount was 1 wt%.

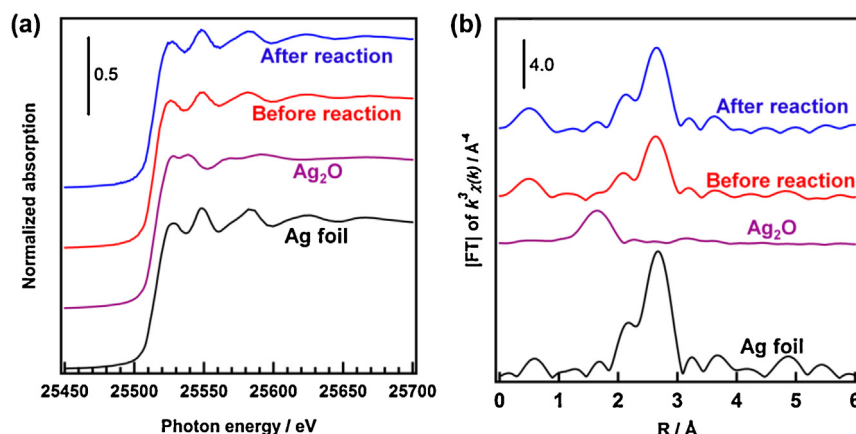


Fig. 9. Ag K-edge XANES (a) and Fourier transformed EXAFS (b) spectra of the optimized Ag-modified La₂Ti₂O₇ before and after the reaction. Ag foil and Ag₂O were references. La₂Ti₂O₇ was calcined at 1373 K for 4 h. Ag cocatalyst was modified by chemical reduction method and the loading amount was 1 wt%.

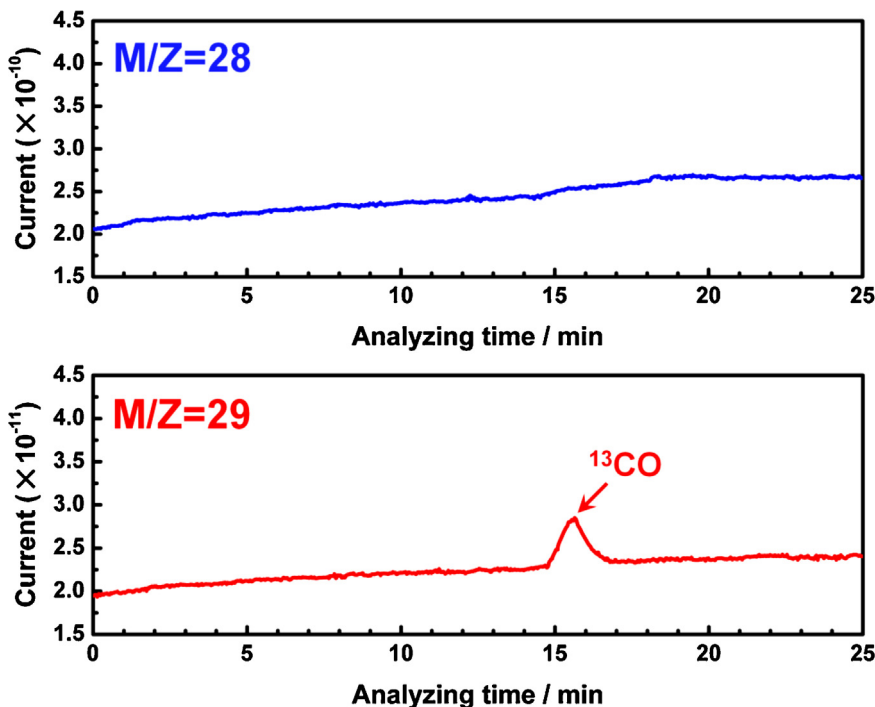


Fig. 11. Mass spectra (m/z 28 and 29) after 5.5 h of photoirradiation in the photocatalytic conversion of $^{13}\text{CO}_2$ in water over Ag-modified $\text{La}_2\text{Ti}_2\text{O}_7$. $\text{La}_2\text{Ti}_2\text{O}_7$ was calcined at 1373 K for 4 h. Ag cocatalyst was modified by chemical reduction method and the loading amount was 1 wt%.

photogenerated holes are consumed by the oxidation of H_2O to produce a stoichiometric amount of O_2 . The equivalence between the reacted electrons and holes confirms that a perfect redox reaction occurred on the surface of Ag-modified $\text{La}_2\text{Ti}_2\text{O}_7$.

Fig. 8 shows the time course of CO, H_2 , and O_2 evolution during the photocatalytic conversion of CO_2 by H_2O over Ag-modified $\text{La}_2\text{Ti}_2\text{O}_7$ under optimized conditions. The evolution rates of CO, H_2 , and O_2 at the steady state (5.2, 4.9 and 5.3 $\mu\text{mol h}^{-1}$, respectively) are in a stoichiometric ratio, indicating that CO_2 is efficiently reduced by H_2O over the Ag-modified $\text{La}_2\text{Ti}_2\text{O}_7$ photocatalyst, and that H_2O is simultaneously oxidized by the generated holes. In addition, CO was produced in priority to H_2 . After 7 h, the amount of evolved CO was 47.7 μmol , which was higher than the amount of evolved H_2 (36.4 μmol). It can be observed that the formation rate of CO declined gradually at the initial stage of the reaction. Fig. 9 shows the Ag K-edge XANES and Fourier-transformed Ag K-edge EXAFS spectra of Ag-modified $\text{La}_2\text{Ti}_2\text{O}_7$ before and after the photocatalytic reaction using Ag foil and Ag_2O as references. The XANES spectra of the Ag-modified $\text{La}_2\text{Ti}_2\text{O}_7$ before and after the reactions were similar to that of Ag foil, implying that the Ag species remained as metallic Ag after the photocatalytic reaction. In the corresponding EXAFS spectra, the height of the Ag–Ag shell peak increased after the photocatalytic reaction, indicating that the particle size of the Ag cocatalyst on the surface of $\text{La}_2\text{Ti}_2\text{O}_7$ became larger after the reaction. Moreover, the grown Ag particles after the reaction can be distinctly observed in TEM images as shown in Figure S2. The change in the Ag particle size is attributed to the redeposition and aggregation of Ag species on the photocatalyst during photoirradiation [14]. This decreased the rate of formation of CO during the initial stage. After 3 h of photoirradiation, the rate became constant. On the other hand, the amount of evolved H_2 and O_2 increased linearly over 7 h of photoirradiation. This means that Ag-modified $\text{La}_2\text{Ti}_2\text{O}_7$ is a very stable photocatalyst for the photocatalytic conversion of CO_2 by H_2O , and is not affected by the oxidation and reduction of the generated hole and electron. The XRD patterns of fresh and recycled Ag-modified $\text{La}_2\text{Ti}_2\text{O}_7$ (Fig. 10) clarified that the crystalline structure of $\text{La}_2\text{Ti}_2\text{O}_7$ after the photocatalytic reaction

was almost the same as that before the photocatalytic reaction. The $\text{La}_2\text{Ti}_2\text{O}_7$ photocatalyst prepared by the polymerized complex method is very stable under UV light irradiation and in aqueous medium.

The $\text{La}_2\text{Ti}_2\text{O}_7$ photocatalyst was calcined at high temperatures in air during the fabrication process; this high-temperature treatment eliminates any carbon residues on the photocatalyst surface. However, it is necessary to confirm the carbon source of the gaseous products such as CO through an isotope-labeling reaction using ^{13}CO to avoid any misestimations in the photocatalytic conversion of CO_2 . Fig. 11 displays the mass spectra (m/z 28 and 29) during the photocatalytic conversion of $^{13}\text{CO}_2$ by H_2O over Ag-modified $\text{La}_2\text{Ti}_2\text{O}_7$ under optimized conditions. Sampling gas was introduced into the mass spectrometer after it was segregated by a gas chromatograph. The peak in the spectrum at $m/z = 29$, which appeared at the same retention time as that observed by GC, can be directly attributed to ^{13}CO gas. The amount of ^{13}CO estimated by mass spectrometry was almost consistent with the amount of CO determined by TCD-GC. This result revealed that the evolution of CO was not from the contamination of $\text{La}_2\text{Ti}_2\text{O}_7$, but from the introduced CO_2 gas.

4. Conclusions

Ag-modified $\text{La}_2\text{Ti}_2\text{O}_7$ exhibited activity for the photocatalytic conversion of CO_2 to CO together with the oxidation of H_2O to O_2 . H_2O functions as an efficient electron donor for the reduction of CO_2 , and the stoichiometric amounts of evolved CO, H_2 , and O_2 indicate that the number of electrons used for the evolution of CO and H_2 is equal to the number of holes consumed for the evolution of O_2 . The photocatalytic activity depends on the crystallinity and surface area of $\text{La}_2\text{Ti}_2\text{O}_7$, which are influenced by the calcination temperature and time. Thus, the maximum amount of CO was produced over $\text{La}_2\text{Ti}_2\text{O}_7$ that was synthesized using the polymerized complex method and calcined at 1373 K for 4 h. The isotope labeling reaction using $^{13}\text{CO}_2$ provided evidence that the evolved CO

did not originate from carbon contamination of $\text{La}_2\text{Ti}_2\text{O}_7$, but from experimentally introduced CO_2 gas.

Acknowledgements

This study was partially supported by a Grant-in-Aid for Scientific Research on Innovative Areas “All Nippon Artificial Photosynthesis Project for Living Earth” (No. 2406) of the Ministry of Education, Culture, Sports, Science, and Technology (MEXT) of Japan, the Precursory Research for Embryonic Science and Technology (PRESTO), supported by the Japan Science and Technology Agency (JST), and the Program for Elements Strategy Initiative for Catalysts & Batteries (ESICB), commissioned by the MEXT of Japan.

Appendix A. Supplementary data

Supplementary material related to this article can be found, in the online version, at <http://dx.doi.org/10.1016/j.apcatb.2014.07.052>.

References

- [1] J. Hansen, L. Nazarenko, R. Ruedy, M. Sato, J. Willis, A. Del Genio, D. Koch, A. Lacis, K. Lo, S. Menon, T. Novakov, J. Perlitz, G. Russell, G.A. Schmidt, N. Tausnev, *Science* 308 (2005) 1431–1435.
- [2] M. Mikkelsen, M. Jorgensen, F.C. Krebs, *Energy Environ. Sci.* 3 (2010) 43–81.
- [3] T. Sakakura, J.C. Choi, H. Yasuda, *Chem. Rev.* 107 (2007) 2365–2387.
- [4] W. Wang, S. Wang, X. Ma, J. Gong, *Chem. Soc. Rev.* 40 (2011) 3703–3727.
- [5] E.V. Kondratenko, G. Mul, J. Baltrusaitis, G.O. Larrazábal, J. Pérez-Ramírez, *Energy Environ. Sci.* 6 (2013) 3112–3135.
- [6] J. Mao, K. Li, T. Peng, *Catal. Sci. Technol.* 3 (2013) 2481–2498.
- [7] A. Kubacka, M. Fernández-García, G. Colón, *Chem. Rev.* 112 (2012) 1555–1614.
- [8] K. Teramura, H. Tsuneoka, T. Shishido, T. Tanaka, *Chem. Phys. Lett.* 467 (2008) 191–194.
- [9] T. Inoue, A. Fujishima, S. Konishi, K. Honda, *Nature* 277 (1979) 637–638.
- [10] I.H. Tseng, J.C.S. Wu, H.Y. Chou, *J. Catal.* 221 (2004) 432–440.
- [11] H. Fujiwara, H. Hosokawa, K. Murakoshi, Y. Wada, S. Yanagida, T. Okada, H. Kobayashi, *J. Phys. Chem. B* 101 (1997) 8270–8278.
- [12] Y. Liu, B. Huang, Y. Dai, X. Zhang, X. Qin, M. Jiang, M.H. Whangbo, *Catal. Commun.* 11 (2009) 210–213.
- [13] S.C. Yan, S.X. Ouyang, J. Gao, M. Yang, J.Y. Feng, X.X. Fan, L.J. Wan, Z.S. Li, J. Ye, Y. Zhou, Z.G. Zou, *Angew. Chem., Int. Ed.* 49 (2010) 6400–6404.
- [14] K. Iizuka, T. Wato, Y. Miseki, K. Saito, A. Kudo, *J. Am. Chem. Soc.* 133 (2011) 20863–20868.
- [15] R. Abe, M. Higashi, K. Sayama, Y. Abe, H. Sugihara, *J. Phys. Chem. B* 110 (2006) 2219–2226.
- [16] J. Kim, D.W. Hwang, H.G. Kim, S.W. Bae, J.S. Lee, W. Li, S.H. Oh, *Top. Catal.* 35 (2005) 295–303.
- [17] Y. Miseki, H. Kato, A. Kudo, *Energy Environ. Sci.* 2 (2009) 306–314.
- [18] H.G. Kim, D.W. Hwang, S.W. Bae, J.H. Jung, J.S. Lee, *Catal. Lett.* 91 (2003) 193–198.
- [19] K. Teramura, S. Okuoka, H. Tsuneoka, T. Shishido, T. Tanaka, *Appl. Catal. B: Environ.* 96 (2010) 565–568.
- [20] Y. Hori, K. Kikuchi, S. Suzuki, *Chem. Lett.* 14 (1985) 1695–1698.
- [21] K.H. Chen, Y.C. Pu, K.D. Chang, Y.F. Liang, C.M. Liu, J.W. Yeh, H.C. Shih, Y.J. Hsu, *J. Phys. Chem. C* 116 (2012) 19039–19045.